

Article

Balanced Foot Dorsiflexion Requires a Coordinated Activity of the Tibialis Anterior and the Extensor Digitorum Longus: A Musculoskeletal Modelling Study

Carlo Albino Frigo ¹, Andrea Merlo ^{2,*}, Cristina Brambilla ³ and Davide Mazzoli ²

¹ Department of Electronics, Information and Bioengineering, Politecnico di Milano, 20156 Milan, Italy; carlo.frigo@polimi.it

² Gait and Motion Analysis Laboratory, Sol et Salus Hospital, 47922 Rimini, Italy; d.mazzoli@soletsalus.com

³ STIIMA, Italian Council of National Research (CNR), 23900 Lecco, Italy; cristina2.brambilla@mail.polimi.it

* Correspondence: ingmerlo@me.com

Featured Application: Awareness of the role of the extensor digitorum longus can point to rehabilitation treatment and functional surgery towards more effective solutions.

Abstract: Equinus and equinovarus foot deviations (EVFD) are the most frequent lower limb acquired deformities in stroke survivors. We analysed the contribution that the tibialis anterior (TA), extensor digitorum longus (EDL) and plantarflexor muscles play in EVFD via a biomechanical musculoskeletal model of the ankle-foot complex. Our model was composed of 28 bones (connected by either revolute joints or bone surface contacts), 15 ligaments (modelled as non-linear springs), and 10 muscles, modelled as force actuators. Different combinations of muscle contractions were also simulated. Our results demonstrate that, compared to the condition when the foot is suspended off the ground, the contraction of the TA alone produces dorsiflexion (from -18° to 0°) and a greater supination/inversion (from 12° to 30°). The EDL alone produces dorsiflexion (from -18° to -6°), forefoot pronation (25°) and calcaneal eversion (5.6°). Only TA and EDL synergistic action can lead the foot to dorsiflexion suitable for most daily life activities ($\geq 20^\circ$) without any deviation in the frontal plane. When pathological contractures of the plantarflexor muscles were simulated, foot deformities reproducing EVFD were obtained. These results can be relevant for clinical applications, highlighting the importance of EDL assessment, which may help to design appropriate functional surgery and plan targeted rehabilitation treatments.

Keywords: dorsiflexion; musculoskeletal modelling; tibialis anterior; extensor digitorum longus; equinus foot deviation; rehabilitation



Citation: Frigo, C.A.; Merlo, A.; Brambilla, C.; Mazzoli, D. Balanced Foot Dorsiflexion Requires a Coordinated Activity of the Tibialis Anterior and the Extensor Digitorum Longus: A Musculoskeletal Modelling Study. *Appl. Sci.* **2023**, *13*, 7984. <https://doi.org/10.3390/app13137984>

Academic Editor: Claudio Belvedere

Received: 16 June 2023

Revised: 3 July 2023

Accepted: 5 July 2023

Published: 7 July 2023



Copyright: © 2023 by the authors. Licensee MDPI, Basel, Switzerland. This article is an open access article distributed under the terms and conditions of the Creative Commons Attribution (CC BY) license (<https://creativecommons.org/licenses/by/4.0/>).

1. Introduction

Stroke is the second leading cause of death, the third cause of disability worldwide and the leading cause of disability in the elderly. The consequences of a stroke depend on the location and size of the lesion. These may involve functional and self-care abilities, speech, vision, spatial perception and several cognitive abilities [1].

Approximately 15 million people worldwide are affected by a stroke yearly, either ischemic or haemorrhagic. Among them, 5 million people remain permanently disabled, and approximately 35% of post-stroke patients develop a severe disability, resulting in a loss of motor functions and/or the impairment of activities in daily living (ADL) [2].

One of the most frequent functional problems that arise over time after a stroke and hinder motor recovery is the onset of muscle overactivity. The prevalence of localised limb spasticity is between 25% and 45% in the first year after a stroke [3–6], depending on the stroke aetiology, and is higher in patients needing to be admitted in acute neurorehabilitation wards [7]. Among the negative consequences of muscle overactivity the development

of muscular–tendinous deformities [8,9] is decisive in developing a negative impact on the patient’s quality of life [10,11]. In particular, the equinovarus foot deviation (EVFD), the most frequent lower limb deviation in stroke survivors [12], can hinder walking ability and, consequently, autonomy. EVFD can cause inadequate foot clearance during the swing phase of gait, thus increasing the risk of falling [10,11]. During the stance phase, EVFD can limit or prevent both the weight-bearing and the progression ability, reducing stability and propulsion [13]. This typically results in the need for assistance and/or the use of orthoses and/or assistive devices [14].

The lack of ankle dorsiflexion and the excessive foot supination that characterises EVFD can result from several levels of weakness, imbalance, overactivity and the contracture of muscles whose tendons surround the ankle joint. The main causes reported in the literature are the overactivity of muscles, weakness of the tibialis anterior (TA) and strength deficits of the peroneus longus (PL) and peroneus brevis (PB) [15,16]. These can sometimes be associated with the contractures and/or spasticity of the triceps surae (TS) and other plantar flexors, including the tibialis posterior (TP), the flexor hallucis longus (FHL) and the flexor digitorum longus (FDL) [10,11,17–22].

Already in the nineteenth century, Duchenne conducted experiments on selective muscle electrostimulation. He clearly described that the action of the extensor digitorum longus (EDL) balanced the TA varus component and favoured neutral dorsiflexion [23]. In the current literature, there is a lack of studies addressing the contribution of EDL weakness in the genesis of EVFD. Only three papers mention the necessity of EDL activity to generate sufficient ankle dorsiflexion during the swing phase.

Reynard and colleagues [24] assessed the balance between the TA and EDL in stroke patients during gait. Conversely to the TA, both the duration and EMG amplitude of EDL activity were reduced when compared to a control group and determined the varus deformity during swing. In their study for the assessment of the equinovarus foot, Deltombe and colleagues [25] stated that the imbalance between the TA and anterior lateral muscles, including the EDL, is responsible for the varus deformity and leads to ankle sprains and falls in stroke patients. Campanini and colleagues [26] reported that an absent or weak EDL activity combined with a normal TA activation during the loading response, pre-swing and swing phases results in EVFD in patients with shortened or inextensible calf muscles. It is noteworthy that studies dealing with the evaluation and treatment of EVFD do not suggest assessing the EDL during walking [16,27]. Skipping this step could negatively influence the choice of EVFD treatment.

In addition, a quantitative analysis of the contribution to balanced foot dorsiflexion of the TA and EDL actions at progressively increasing levels of TS contracture is missing. To investigate this problem, we selected musculoskeletal modelling as an appropriate and effective tool [28–30]. Provided that a proper model is available, every parameter contained within can be controlled, and the effects of different inputs can be carefully analysed. Furthermore, such an approach has been widely applied in the literature dealing with knee and hip orthopaedic pathologies and joint arthroplasty [31–33].

In this study, we created a biomechanical musculoskeletal model of the ankle–foot complex and used it to analyse the contribution of the TA, EDL and plantarflexor muscles in EVFD. Different combinations of muscle contractions were applied with the foot off the ground, and the resulting 3D ankle kinematics were computed. The aim was to verify, from a purely biomechanical point of view, the combined effect of EDL weakness or paresis and the plantarflexor contracture on ankle dorsiflexion.

2. Materials and Methods

We developed a foot–ankle model composed of 28 bones mutually interacting through specific joint constraints with either revolute joints or bone surface contacts. The modelling platform was SimWise-4D (Design Simulation Technologies, DST, Canton, MI, USA) which allows for simulating the forward and inverse dynamics of complex articulated systems. The integration algorithm was based on the Kutta–Merson process. The follow-

ing parameters were adopted: integration step 0.02 s, configuration tolerance 0.01 mm and 0.1 deg. Fifteen ligaments, modelled as springs with a non-linear characteristic, and 10 muscles, modelled as force actuators, were included in the model (Figure 1). All the details pertaining to joint modelling, ligaments characteristics and muscles are described in the Supplementary File.

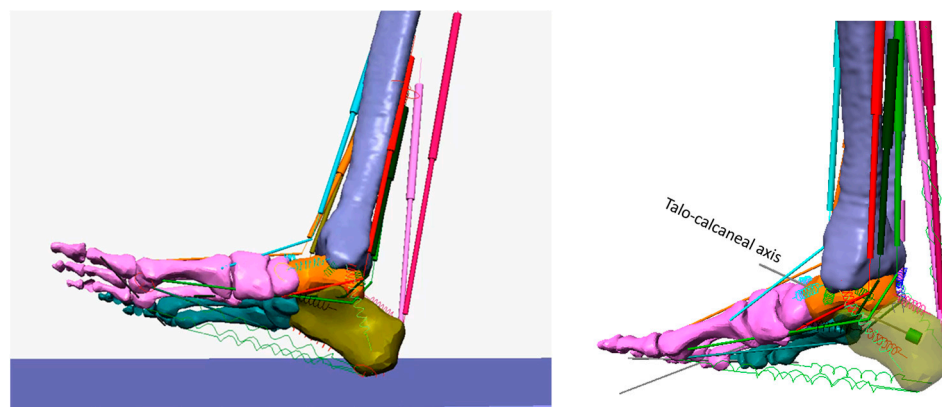


Figure 1. The foot model. The different bones are coloured differently: pink the medial side of the foot (first three rays); blue/green the lateral side (4th and 5th rays); orange the astragalus; green/brown the calcaneus; blue/violet the tibia and peroneus. The linear actuators represent the muscles: pink the soleus; red the gastrocnemius and the tibialis posterior; green the flexor hallucis longus; dark green the flexor digitorum longus; light blue the tibialis anterior, and orange the extensor digitorum longus.

The digital models of the bones were obtained by segmenting MR images extracted from our repository. The data refer to a healthy Caucasian male (age: 42 years, body height: 1.72 m, body mass: 70 kg). The software employed for the image segmentation was Amira (Amira 5.3.3, Visage Imaging, Inc., San Diego, CA, USA).

Among the 10 plantarflexor and dorsiflexor muscles (see Supplementary File), the tibialis anterior (TA), extensor digitorum longus (EDL) and soleus (SO) were selected as the most pertinent for our purpose. The TA and EDL were selected because they are synergistic as dorsiflexors but have a different role in the frontal plane, while the SO was chosen to model the triceps surae muscle. All muscle models included the tendon component without distinction from the contractile component, forming the muscle–tendon unit.

2.1. Foot Angles Definition

Our model allowed us to measure any movement pertaining to the foot bones. Properly identifying the reference axes is essential to identify the angles deserving clinical attention.

We concentrated our attention on the following joint angles:

- The forefoot dorsiflexion/plantarflexion angle and forefoot supination/pronation angle. A mediolateral axis, fixed to the distal tibia and passing through the centre of curvature of the tibial trochlea, was adopted as the dorsi/plantarflexion axis (see revolute joint A in Figure 2). A bar (labelled L in Figure 2), representing the longitudinal axis of the foot, was connected to revolute joint A, while the other extremity of the bar was connected to the forefoot. Since the bar could only move in a plane perpendicular to the dorsi/plantarflexion axis, the connection with the forefoot was defined as follows: a transverse bar labelled F was connected to the first and fifth metatarsal heads through constraints that allowed medial–lateral and distal–proximal translations and all the three pertaining rotations. These were named the ‘sphere on plane’ constraints. The transverse bar F was then connected to bar L by a revolute joint (labelled D in Figure 2) which was oriented on the longitudinal axis of the foot. In this way, the pronation/supination and other movements out of the sagittal plane were not constrained by our measuring system. The rotation of bar L about the dorsi/plantarflexion axis was measured by revolute joint A, and was defined as

the ‘forefoot dorsiflexion’ angle. The rotation of transverse bar F about the longitudinal axis of the foot was measured by revolute joint D, and was named the ‘forefoot supination’ angle.

- Talotibial rotation angle. A bar labelled T was hinged to revolute joint A and connected to the talus through a ‘sphere on plane’ constraint (see above). Bar T acts as a reference axis for the talus. Revolute joint A provided us with the talotibial rotation angle.
- First metatarsus–talus rotation angle. A mediolateral axis passes through the centre of the talonavicular joint (talonavicular axis). Revolute joint C (see Figure 2) was designed to measure the dorsi/plantarflexion angle of the first metatarsal bone in relation to the reference axis of the talus (parallel to bar T). A bar (labelled M in Figure 2) was hinged to revolute joint C and connected to the first metatarsal bone by a sphere on plane constraint. The angle measured by revolute joint C was named the ‘first metatarsus–talus’ rotation angle.
- Calcaneus inversion/eversion angle. The axis of rotation of the talocalcaneal joint, the Henke axis [34], was identified as an axis passing through the superior part of the talus and the lateral tuberosity of the calcaneus. When the foot was on the ground, the talocalcaneal axis was oriented at 42° over the horizontal plane and 16° medially about the longitudinal foot axis. The corresponding revolute joint (labelled B in Figure 2) was fixed to the talus and provided us with the relative rotation of the calcaneus about the talus (the calcaneus inversion/eversion angle).

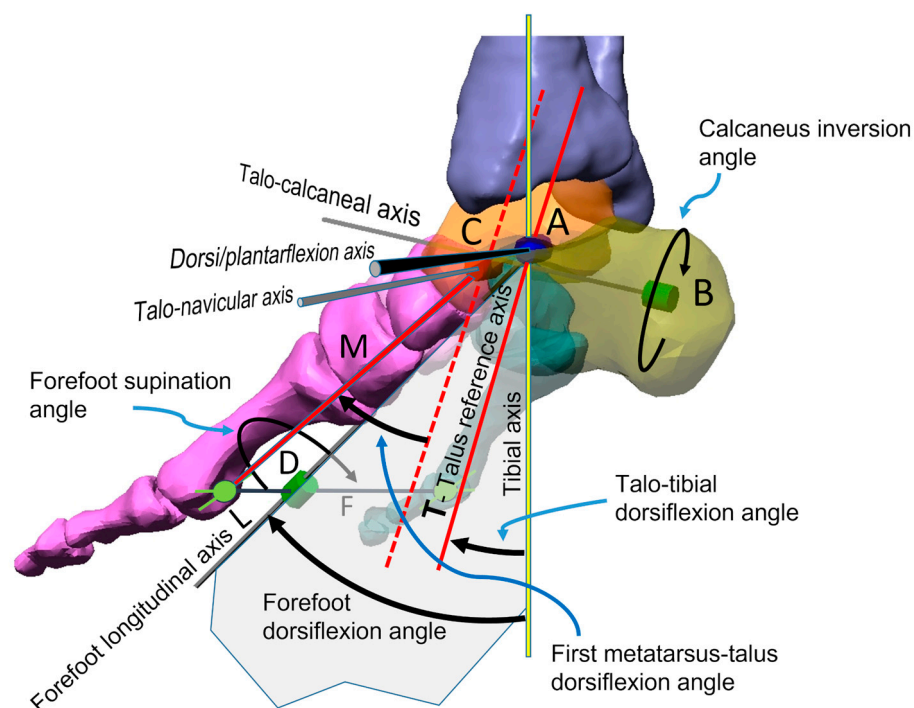


Figure 2. Foot axes and angles as defined in the model used in this study. Letters A, B, C, D indicate the revolute joints which allow the rotation around the Dorsi/plantarflexion axis (A), the Talo-calcaneal axis (B), the Talo-navicular axis (C), the Forefoot longitudinal axis (D) respectively.

2.2. Foot Unloading

At first, the model was allowed to adjust to a flat surface by applying a non-penetrating constraint between the foot bones and the ground and allowing the tibia to slide freely along the vertical axis while keeping a vertical orientation. No loads were applied, and only the gravitational force acted on the structures. This arrangement, with the foot resting on the floor and free of any load, was used as the reference condition—i.e., the corresponding foot angles were considered as the zero reference angles.

Later, the foot was lifted off the ground by applying an upward vertical shift to the tibia. Again, no muscle force was applied, and the foot hung to the tibia in a position set only by gravity and passive ligament tension. This was the initial setup for the subsequent simulations.

2.3. Simulated Muscle Contractions in Normal Conditions

Muscle contractions were simulated by applying a predefined shortening velocity on the force actuators. To avoid any brisk accelerations and the confounding effects of inertia, especially at the initial phases of movement, the shortening velocity had to be relatively low (quasi-static condition). On the other hand, low velocity entails an increase in the computational time. A compromise was deemed acceptable with a shortening rate of 2 cm/s (the simulation time was approximately 6 min). The force produced by the force actuators during shortening was also monitored.

We analysed the effect of muscle contraction both individually (the TA as the main dorsiflexor and invertor muscle, and the EDL as the main dorsiflexor and evertor muscle) and jointly (TA + EDL). The effect of the extensor hallucis longus (EHL), which is synergistic with TA for dorsiflexion and inversion, was not investigated in this study because of its complex multi-joint function. This would have required a more complex model and was outside the scope of the present work. The resistance to dorsiflexion due to soft tissue and the passive properties of the plantarflexor muscles was modelled using the exponential equation proposed in [35]. The corresponding resistive force, which is exponentially subordinate to the dorsiflexion angle, was inputted into the actuators representing the gastrocnemius (GA) and soleus (SO). We analysed the ankle joint movements resulting from these conditions along with the SO lengthening (ΔL_{SO}) corresponding to full dorsiflexion.

2.4. Simulated Muscle Contractions in Stroke-Like Conditions

The effect of calf muscle-reduced extensibility was analysed in a series of simulations in which the SO lengthening was limited to 75%, 50% and 25% of ΔL_{SO} . For ease of clarity, 75% ΔL_{SO} represents a mild limitation, while 25% ΔL_{SO} represents a severe one. In stroke patients, reduced muscle extensibility typically results from increased intrinsic stiffness and pathological muscle activity in response to tension, stretching or a combination of the two [36]. The three limiting values were selected to model the progression of TS alterations between the pre-stroke physiological conditions ($\Delta L_{SO} = 100\%$) and a fixed contracture ($\Delta L_{SO} = 0$) [37,38].

These limitations imposed on SO inhibit the calcaneus movement in the sagittal plane and could also represent the distal effect of the gastrocnemius (GA) shortening. For this reason, we deemed it unnecessary to simulate the gastrocnemius contracture separately. Other plantar flexor muscles, such as tibialis posterior (TP), were not analysed because of their multi-joint function, which could have made the interpretation of the results more complicated. TA, EDL and TA + EDL contractions were simulated as in the previous case, and muscle forces and foot angles were measured in all these shortened conditions.

3. Results

3.1. Initial Model Condition

Once the foot was lifted off the ground and after a few oscillations, it stabilised in a slightly plantar flexion position (-18 degrees) with a mild forefoot supination (12 degrees), as shown in Figure 3.

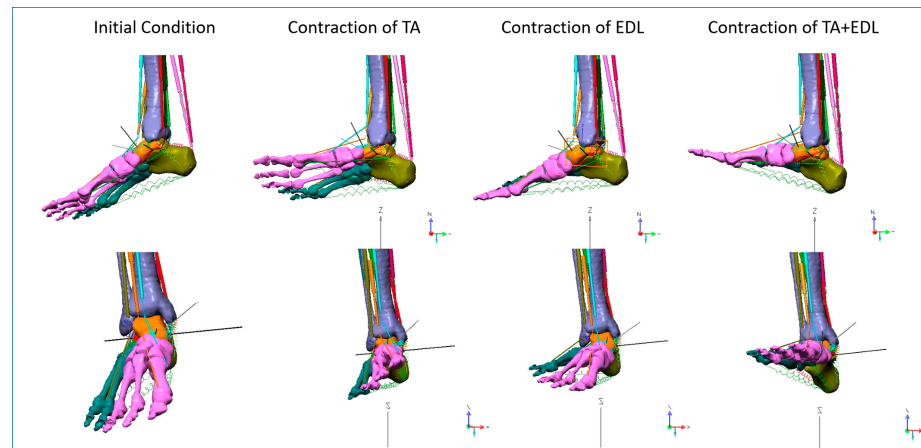


Figure 3. Configurations of the foot model as obtained at the beginning (leftmost column) and at the end of the different simulations. **Above:** sagittal view; **Below:** frontal view.

3.2. Maximum Muscle Shortening

Beginning with the above-mentioned position, muscle contractions were applied. These produced a movement of the foot consistent with joint kinematics and ligament constraints. The simulations were stopped when abnormal deformations started to appear. This happened quite early when EDL was actuated (contracted) alone (see Figure 4). In this condition, the EDL shortening was 16.8 mm, while SO lengthened by 7 mm (panel G). TA contraction did not produce abnormal deformations until it shortened by 24.8 mm, corresponding to a SO lengthening of 14.9 mm. The simultaneous contraction of the TA + EDL allowed the foot to dorsiflex until the two muscles were shortened by 29.6 mm and the SO was lengthened by 24.2 mm.

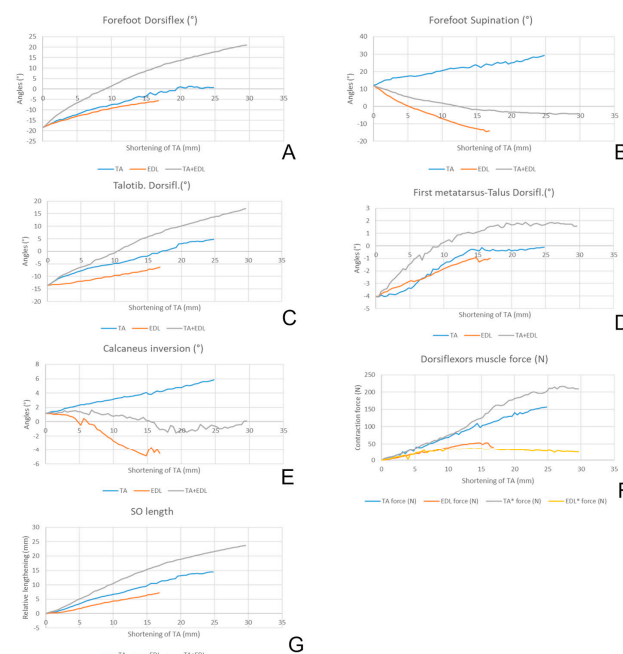


Figure 4. Foot joint angles (panels A–E), dorsiflexors muscle force (F) and SO muscle length (G) during shortening of the TA (blue), EDL (orange) and both TA + EDL (grey). In (F), the forces TA* (grey) and EDL* (yellow) correspond to when the TA and EDL were simultaneously contracted. The horizontal axis refers to time. The curves have different durations because the simulation was stopped when inconsistent deformations of the foot started to appear. That happened early when the EDL was contracted alone, then when TA was contracted alone and later when both muscles were contracted simultaneously.

3.3. Effect of TA, EDL and TA + EDL Contraction on Dorsiflexion

Figure 3 shows the positioning of the foot model obtained when the foot was hanging freely and prior to placing muscle forces and at the end of TA, EDL and TA + EDL simulated contractions.

The activation of TA alone produced very mild dorsiflexion, while forefoot supination was the most relevant movement. On the contrary, the activation of the EDL determined forefoot pronation but still negligible dorsiflexion. Only the simultaneous and balanced activation of both TA and EDL produced dorsiflexion and negligible pronation/supination. The analysis of the foot joint angles confirms this qualitative observation (see Figure 4). The range of motion obtained for each of the angles considered is summarised in Table 1.

Table 1. Amplitude of the movement obtained by the simulated contraction of the TA, EDL and TA + EDL. The first column reports the angles at the beginning of the simulation when the foot was suspended off the ground.

Joint Rotation	Initial Condition	TA	EDL	TA + EDL
Forefoot dorsiflexion	−18°	18°	12°	39°
Forefoot supination	12°	18°	−25	16°
Talotibial dorsiflexion	−13.5	18.5°	6°	30.5°
First metatarsus–talus dorsiflexion	−4°	4°	3°	5.6°
Calcaneus inversion	1.2°	4.8°	−5.6°	−3°

When TA and EDL contracted separately, the muscle forces at the end of the movement were 152 N for the TA and 50 N for the EDL. When both muscles were contracted simultaneously, the force was 210 N and 25 N, respectively.

Figure 5 presents the effects of limiting the length excursion of the SO during the contraction of TA. The following effects could be observed:

- Foot dorsiflexion produced by the TA was progressively limited as far as the SO was constrained to shorter excursions. After that limit, the effect of the TA contractions switched from dorsiflexion to plantarflexion (panel A);
- Forefoot supination increased more rapidly as soon as the SO length achieved its limit (panel B);
- Talus dorsiflexion about the tibia was stopped while the first metatarsus increased in dorsiflexion (panels C and D);
- The calcaneus inversion increased more rapidly (panel E);
- The force of the TA increased considerably as long as the SO lengthening was reduced.

Figure 6 presents the effects of limiting the length excursion of SO during the simultaneous contraction of the TA and EDL. These effects can be described as follows:

- Foot dorsiflexion slows down and comes to a stop as the limitation of the SO lengthening progresses (panel A);
- Forefoot pronation and the talotibial dorsiflexion stop at different angles in correspondence with the SO lengthening limitation (panels B and C);
- Dorsiflexion of the first metatarsus is affected differently at the beginning of the movement (SO lengthening limited at 25%) than at the end (SO lengthening capped at 75%). In the former case, dorsiflexion increased; in the latter, dorsiflexion lessened (panel D);
- The calcaneus undergoes a sharp inversion as soon as the SO lengthening stops (panel E);
- The contraction force of both the TA and EDL abruptly increases when SO lengthening is halted (panels F and H).

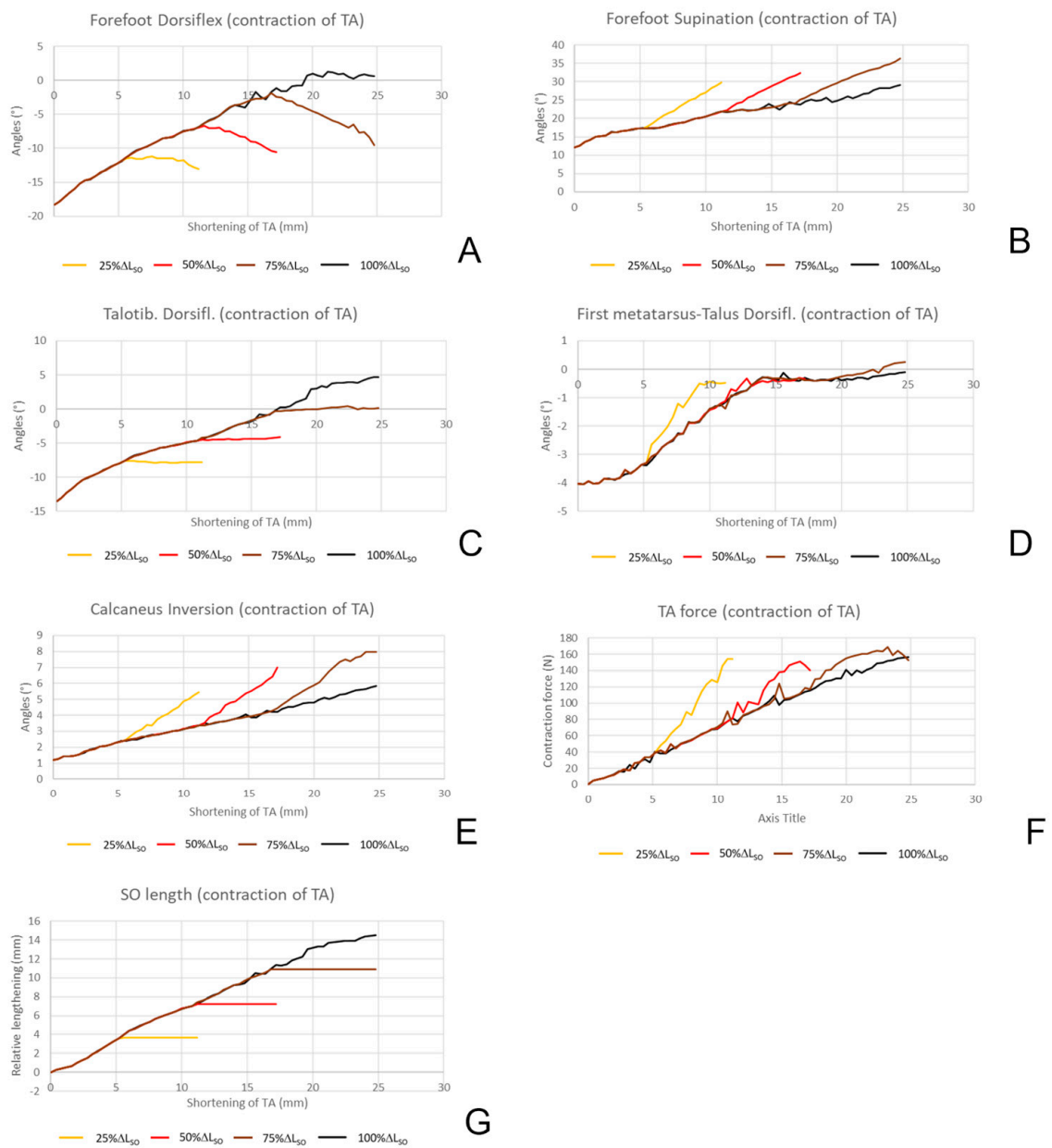


Figure 5. The effects of limiting the length excursion of the SO during the contraction of the TA. Different colours represent the effect of different allowed length excursions: from 100% (black curve), indicating no limitation, to 25% (yellow curve), indicating that the SO can only lengthen by 25% of its full range. Foot joint angles are reported in panels (A–E), dorsiflexors muscle force in (F), SO muscle length in (G).

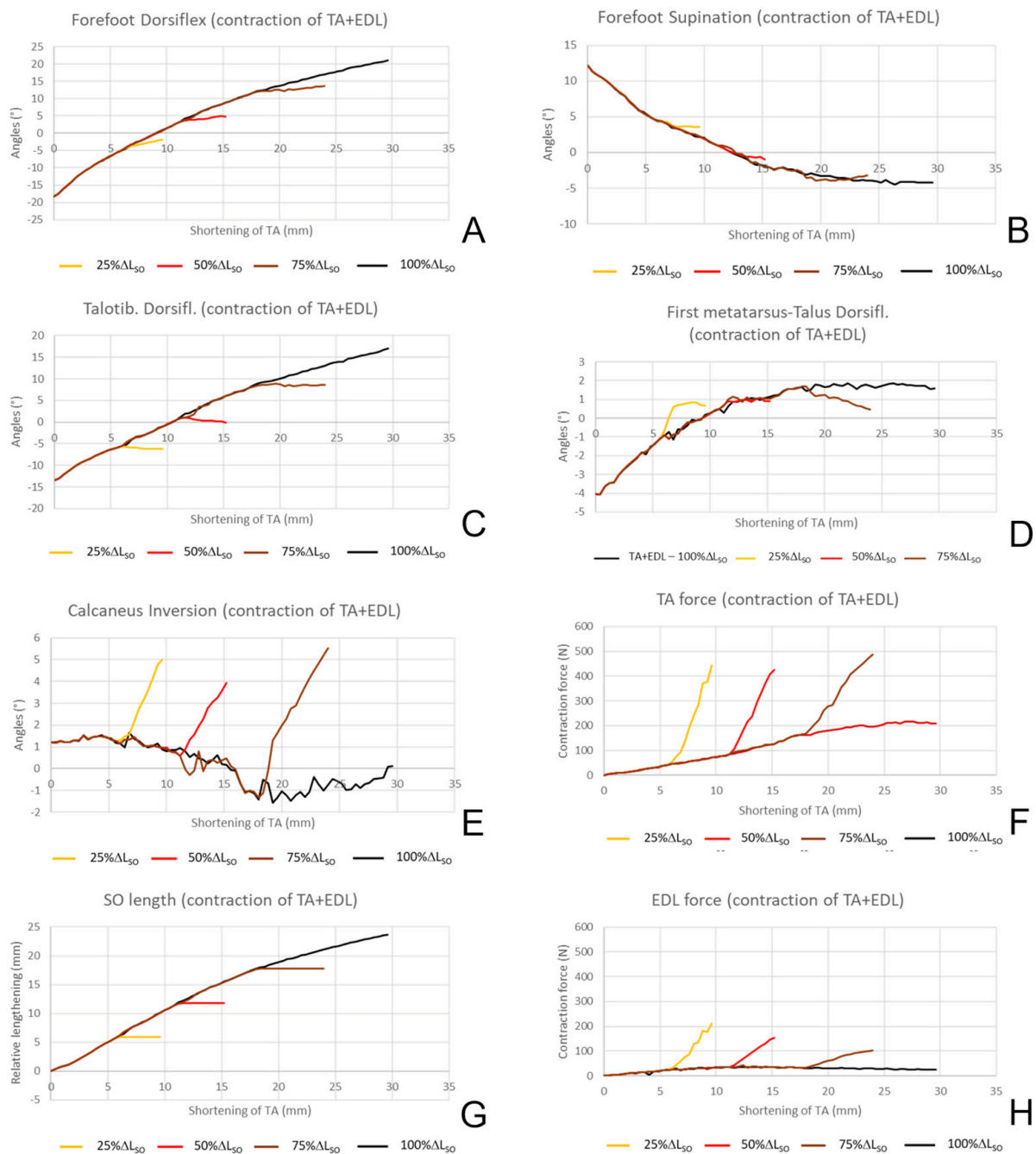


Figure 6. The effect of limiting the length excursion of the SO during the simultaneous contraction of the TA and EDL. Different colours represent the effects of different length excursions from 100% (black curve), indicating no limitation, to 25% (yellow curve), indicating that the SO can only lengthen by 25% of its full range. Foot joint angles are reported in panels (A–E); TA force and EDL force are reported in panels (F) and (H) respectively; SO muscle length in (G).

4. Discussion

In this study, we analysed the contribution that the TA and EDL have on foot dorsiflexion and pronation and supination through a biomechanical simulation of the foot–ankle district. We simulated both normal conditions and a set of conditions typical in stroke patients. Our aim was to quantify to what extent dorsiflexion was affected by these two muscles and to promote awareness among clinicians of the key role played by the EDL in stroke patients with EVFD.

In the model, the TA was considered because it is the main dorsiflexor muscle that inserts on the medial surface of the foot. EDL was included in the model because it is the main dorsiflexor muscle that inserts on the lateral surface of the foot.

The results of our modelling study demonstrate that dorsiflexion is only achievable through the synergistic and balanced action of the TA and EDL. Specifically, the contraction of the TA or EDL alone cannot lift the foot beyond the neutral sagittal position (0 degrees). This condition does not allow foot clearance during swing [39], which is one of the prerequisites of normal gait [40]. The lack of dorsiflexion typically results in the adoption of compensatory mechanisms to move the trailing limb forward, such as pelvic elevation and greater hip and knee flexion in the sagittal plane or the lateral bending of the trunk and limb circumduction in the frontal plane.

In the clinical field, functional electrical stimulation in patients with drop foot shows similar results. Proper stimulation of both the TA and EDL is required to achieve a balanced foot dorsiflexion [41,42]. Taken individually, neither muscle can produce neutral dorsiflexion, i.e., without deviations in the frontal plane and with a magnitude suitable for most daily activities. In stroke patients with EVFD (with normal TA activity and missing EDL measured by surface electromyography), a surgical procedure named SPLATT (split tibialis anterior tendon transfer) and calf muscle lengthening are often recommended [43]. In SPLATT, the TA tendon is cut longitudinally into two parts; one branch remains in place, and the other is transferred to the lateral side of the foot and fixed to the cuboid. This provides a mechanical contribution similar to that which the paretic EDL can no longer provide.

Our results highlight the contribution of the TA and EDL to ankle joint rotation in both the sagittal and frontal planes. Starting with the foot hanging freely, the TA contraction alone determined up to 18 degrees of dorsiflexion (from -18° to 0°). This brought the ankle back to a neutral position without further dorsiflexion. Despite being commonly known as the main dorsiflexor muscle, the main action of the TA (alone) is to produce foot supination. In our study, when only the EDL was contracted, it rotated the ankle by 12 degrees into dorsiflexion (from -18° to -6°) and the foot shifted into pronation (see Figure 4). Only the combined contraction of the TA and EDL resulted in the physiological dorsiflexion peak (e.g., 15 degrees) needed for walking and with the foot neutral in the frontal plane. Textbooks used as reference by students and clinicians alike also indicate that the EDL is a muscle that assists foot dorsiflexion and counteracts supination [44,45]. Nevertheless, when addressing a lack of foot dorsiflexion, studies only take into account the TA and seldom consider the EDL and its role during walking, e.g., in stroke patients. There seems to be little awareness of the EDL's fundamental role in achieving balanced dorsiflexion during the pre-positioning of the foot on the ground and providing foot clearance during the swing phase of gait. With the support of the simulation results presented in this study, we would like to emphasise the importance of measuring EDL activity during the gait of EVFD patients.

Most of these patients typically present several combinations of overactivity and shortening of the plantarflexor muscles. This antagonises the mechanical effect of the dorsiflexors, inevitably leading to the equinus deviation [26]. In our study, we mimicked this outcome by gradually shortening the SO. Our simulations show that even a mild reduction in SO extensibility is sufficient to prevent adequate foot dorsiflexion, which cannot reach the neutral position (Figure 5A). Most likely, this could result in an increased risk of stumbling during walking and may induce the subject to compensate for such limitations by adopting strategies involving other lower limb districts [14,43–45]. Therefore, from a clinical perspective, maintaining the length and extensibility of the triceps surae must be a priority for rehabilitators to be considered already in the acute phase after a stroke [46].

Looking at Figure 5A, it may be surprising to see plantarflexion occurring during TA contraction as soon as the limit of the SO length is achieved. To explain this paradox, it must be noted that TA shortening causes forefoot supination and calcaneus inversion

(Figure 5B,E). The force needed to shorten the TA increases abruptly (Figure 5F). The calcaneus inversion occurs about the talocalcaneal axis, while the forefoot supination results from a combination of movements about the talonavicular joint and the cuboid–calcaneal joint. The association of these two movements produces the supination and adduction of the forefoot. With the foot supinated and adducted, the part of the foot intersecting the plane where the dorsi-plantarflexion angle is measured is the lateral side. Since during supination the first metatarsus moves upwards and the fifth metatarsus moves downwards, the angle measured in that plane corresponds to plantar flexion. Figure 7 can help us better understand this phenomenon. This situation is common with neurologic patients (e.g., after a stroke). The upward movement of the first metatarsal head following foot supination should not be interpreted as mild dorsiflexion since the foot crawls on the floor in this case.

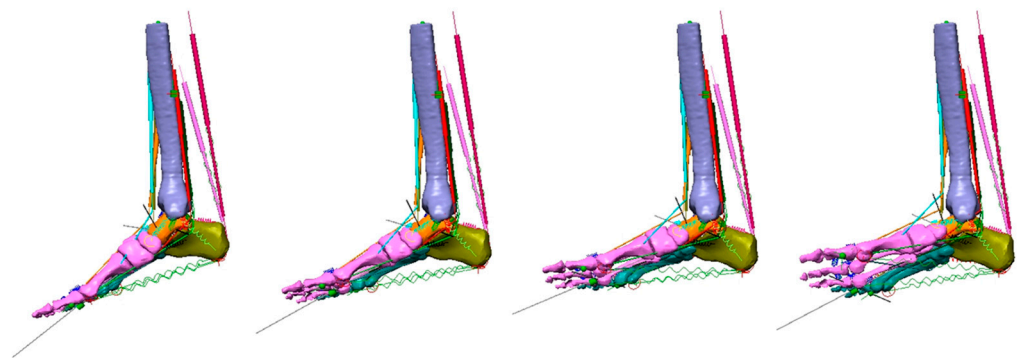


Figure 7. From left to right: progressive dorsiflexion until the SO stops lengthening, and foot inversion occurs associated with plantarflexion of the lateral side of the foot. In this example, SO lengthening was limited to 75%.

When considering the combined contraction of the TA and EDL, the forefoot supination is prevented by the balanced activity of these two muscles.

When SO extensibility is limited, their action results in calcaneus inversion. This can be seen in Figure 6E). Of course, this mechanical solution entails a considerable increase in the TA and EDL force (panels F, H) and is necessarily limited to a small degree of foot dorsiflexion (panel A).

It is worth mentioning that we simulated the effect of plantarflexor contracture by exclusively limiting the length excursion of the SO. This may appear oversimplistic since the resistance to foot dorsiflexion can be caused by several other factors: increased muscle stiffness, increased muscle viscosity and muscle overactivity [37,38]. However, they all result in a hindrance to the normal length excursion. Our data tested different degrees of length limitation, and it can provide insight into the effects of such a phenomenon.

4.1. Modelling and Validation

The model used in this study is “length-controlled”. This means that the shortening of a muscle was set and all other variables such as joint angles, bone segments orientation and forces were obtained as a result. The selected shortening velocity was -2 cm/s and corresponded approximately to an angular velocity of 20° /s in dorsiflexion. This value is comparable to the velocity at which voluntary dorsiflexion is performed during selective tests at the bedside [47]. It should be remembered, though, that the choice of this shortening velocity was not intended to replicate a physiologic condition (e.g., the peak of dorsiflexion velocity occurring during walking, which is in the order of 100° /s—approximately 20° in 0.2 s after foot-off). Our intention was to avoid sharp accelerations and the corresponding inertia forces that would have tainted the muscle contractions, particularly at the beginning of the movement. On the one hand, the shortening velocity adopted is slower than the physiological one required for dorsiflexion during activities such as walking. On the other hand, our model contains neither dampening elements (e.g., capsule, muscle viscosity) nor

reflex activations (e.g., spasticity) and so the forces and the resulting movement do not depend on the value of the shortening velocity. Because of the lack of elements sensitive to the dorsiflexion velocity, i.e., muscle viscosity and muscle spasticity, our model does not fully represent the complex biomechanics of ankle dorsiflexion. In this regard, it is reasonable to suppose that phenomena limiting the triceps surae extensibility would lead to deviations similar to those modelled in this study, where TS extensibility was limited at four discrete levels. However, this would require a specific simulation that was out of the scope of our study.

In our simulations, muscle forces achieved (210 N for the TA) are all within a range of feasibility. An interesting paper by Maganaris [48] reports, in a controlled stimulation condition, a range of TA force from 157 \pm 19 N to 644 \pm 88 N. Similarly, data reported by Lenhard [49] show a maximum voluntary dorsiflexion force of approximately 300 N, measured by a force sensor positioned on top of the metatarsal heads. If the lever arm of the force were twice the lever arm of the muscle dorsiflexors as a whole, the dorsiflexion force would be approximately 600 N. No reference data were found for EDL. Still, one can ponder on the relative strength that can be inferred by considering the physiological cross-sectional area (PCSA) of the two muscles. Friedrich and Brandt [50], in a cadaver dissection study, reported a PCSA of 16.88 cm² for the TA and 7.46 cm² for the EDL, corresponding to 44% of the TA PCSA. The maximum force we obtained for the EDL was 50 N, less than 24% of the TA force. We can thus confirm that even for the EDL, the forces obtained in our simulation were far below the maximum force capacity of this muscle. With regard to the numerical solution stability, it is worth noting that even dramatically altering the muscle forces (the alternative removal of the TA or EDL, different limitations of the SO length excursion), the software was able to proceed in the simulations and compute the corresponding changes in foot movements. Of course, an overall assessment of the accuracy of the results was impossible since it is impossible to obtain a controlled contraction of one single muscle in a real individual. Consequently, we were unable to obtain any real reference data. The movements obtained were consistent with the limits imposed by the ligaments (i.e., having non-linear behaviour), the joint surfaces and the axes of rotation, and the movement amplitude was progressively increasing along with the muscle forces. We are therefore confident that the relevant effects of the different muscle configurations are accurately reproduced by the model. The accuracy of our simulations strongly depends on the accuracy and reliability of the structural and functional parameters of the model (bone morphology, functional axes, degrees of freedom) and on the input variables (the variables that reproduce muscle contractions). Although the solutions adopted are based on consolidated knowledge and relatively sophisticated technologies, further investigations are advisable to increase the reliability of the model and make it suitable for many other applications. For example, the mechanical properties of the specific foot ligaments and other soft tissues (cartilage, plantar fasciae, capsulae) should be better identified to increase the reliability of the model. Muscle viscosity and possibly reflex activations should be modelled. Deep investigations of the real behaviour of the foot during movement and in natural loading conditions would be useful to improve the possibility of simulating more complex motor acts such as walking and different gait types.

4.2. Clinical Implications

An accurate analysis of the isolated actions of TA and EDL, associated with simulations of frequent pathological conditions in patients, such as the muscular-tendinous shortening of SO, can provide useful information when planning corrective interventions [26].

The aim of this paper was to increase clinicians' and researchers' awareness of the key role EDL plays in the development of EVFD. In our opinion, professionals should start considering the assessment of EDL as important as that of TA.

Being aware of the mechanical effects of both muscle activation and calf muscle shortening could help professionals design tailored rehabilitation interventions for their patients. When EDL activity is still weakly present during walking, rehabilitation should

focus on strengthening the EDL through therapeutic exercise associated with electrical stimulation. Conversely, when the EDL cannot be recruited during walking, an orthosis or neuro-orthopaedic surgery (e.g., SPLATT) should be selected according to the patient's goals and overall assessment. Neuro-orthopaedic (or "functional") surgery is, in general, an effective treatment for managing chronic deformities in neurologic patients. It restores musculoskeletal balance through precision interventions such as tendon transfers, muscle-tendon lengthening and aponeurectomies [26,39,43].

In addition, given the demonstrated influence of triceps surae contractures on foot movements, it would be advisable to implement an early treatment of this muscle, thus preventing the onset of structured rheological alterations. Physiotherapists can provide patients with prolonged stretching and instrumental therapies, such as shock waves or dry needling [51]). Support orthoses can then be added in order to support the most deficient or weak districts. The contribution of surface electromyography (sEMG) can be decisive in choosing the most appropriate treatment according to the patient's needs [26].

Our simulations show how SO contractures can alter TA activity, determining increased supination instead of the desired dorsiflexion. In patients with this contracture, sEMG measurements often show a continuous activity of TA. This is reasonably an attempt to contrast the SO brake, not a pathological activity [26]. In light of the present analysis, the instrumental assessment of EDL activity in the presence of equinus or equinovarus foot deformity is advisable.

4.3. Limitations

Given the extremely complex structure of the foot, a compromise had to be reached between the need to represent the phenomena of interest and the need for simplification. However, there is a need to improve the knowledge of the mechanical properties of specific components of the foot structure and the computational capacity of the simulation software in order to increase the complexity of the model, make it more realistic and improve the validity of its predictions. In this study, we were interested in the movement and foot configurations produced by the TA and EDL. Hence, we deemed it necessary to represent the main joints as accurately as possible. This was obtained by modelling the interaction of joint surfaces (the tibiotalar joint), the predefined 3D oriented rotation axes (the talocalcaneal and the cuboid–calcaneal joints) and by applying spherical constraints when necessary (the talonavicular joint)—see Supplementary File. Instead, for the sake of convenience, the navicular, cuneiforms and the first three metatarsi were considered to be rigidly connected, forming a single unit for the medial forefoot, while the lateral forefoot included the cuboid and fourth and fifth metatarsi. For the toes, only the metatarsal–phalangeal joints were represented by revolute joints. These were the main structural limits of our model. These were not supposed to influence the effects of TA and EDL activity on the ankle joint. Other somewhat questionable choices were the positioning and the mechanical characteristics of the foot ligaments. We tried to represent the ligaments according to the anatomical descriptions in specific biomechanical studies [52–56]. However, because of discrepancies between different authors on ligament mechanical characteristics, we had to adapt the literature data to our specific model. Nevertheless, since the movements obtained under different loading conditions were quite realistic and within the physiological range of motion, we are confident that the adopted parameters were mostly correct. For the muscles, we considered the muscle–tendon complex as one (i.e., without separation between contractile and tendon components), since it did not change nor alter the force transmitted at the insertion point.

The direction of that force is important, though, and for this reason we have represented the via-points constituted by the retinaculum, which forces the tendons of the TA and EDL to remain close to the tibial bone. As to the plantarflexors, both the SO and the gastrocnemius muscles were taken into consideration, but their contracture was simulated simply by limiting the length excursion of the SO. Since these two muscles act on the same tendon (the Achilles tendon), the limits imposed on just one of them are representative of the contracture of the whole group. Other calf and foot muscles could have been con-

sidered, but the complexity of their interaction with synergistic and antagonistic muscles would have required a more in-depth investigation, and this was beyond the scope of the present study. For the same reason, the EHL was not analysed separately. It works synergistically with TA but has a smaller cross-sectional area and lever arm. This results in smaller dorsiflexion and inversion moments. Moreover, it has additional effects on the first metatarsal–phalangeal joint. Tibialis posterior was not included in our model. Hence, its contribution to EVFD was not tested. Moreover, we did not model any reflex circuit and, consequently, TS spasticity. Rather, we modelled the limited extensibility of the calf muscles that can result from TS spasticity.

It is worth noting that we presented the results based on the anatomical characteristics of a single subject. A sensitivity analysis on the effects that a variation in each moment arm value has on the computed angle, as in [57], is missing. Future studies should analyse a wider range of scenarios or input conditions, thus being representative of the samples of subjects instead of one single healthy adult.

The objective was not to develop a model to predict the actual dorsiflexion in a specific patient but, as stated in the introduction, to highlight the importance of the activation of the EDL muscle for dorsiflexion, since this muscle is often neglected in the rehabilitation of neurologic patients. If we had to develop a patient-specific model, we had to consider that most parameters depend on sex, age, body size, body mass and specific anatomic and clinical conditions. There is not enough information at present to achieve this goal, but the objective of a patient-specific model is one of the main aims of research in this area.

The passive alterations of muscle properties that lead to a failure in muscle lengthening can be caused by structural shortening (e.g., a decrease in the number of sarcomeres), increased stiffness and viscosity. Stiffness and viscosity act as the velocity-independent and velocity-dependent components of the resistance to stretching [37,38]. In our model, all these phenomena were represented by limiting the SO muscle lengthening at various levels. Since the length variation of the active muscles (the TA or EDL or both) was imposed, the resulting forces could reach very high values, and the foot would seriously deform. This is what we observed in Figures 5 and 6. If the limitation of the SO stretch had been progressive, we would have observed a more gradual increase in the forces and a gradual decrease in foot motion. If that were the case, the effect of muscle contracture would have been less evident and, therefore, less useful for our goal. To avoid misinterpreting the results, our simulations were halted when the TA or EDL contractions became excessive (i.e., non-physiological).

5. Conclusions

Our study is based on musculoskeletal modelling. It showed that a combined activity of TA and EDL, along with appropriate extensibility of the triceps surae muscle–tendon unit is required to achieve a useful and balanced ankle dorsiflexion, suitable for walking. EDL paresis and weakness, which are common in patients with an upper motor neuron lesion, result in foot supination with no or very limited dorsiflexion, even in the presence of normal TA activity. Similarly, dorsiflexor muscle activation in the presence of a contracture of the calf muscles results in foot supination, along with the expected lack of ankle dorsiflexion. These findings can be useful for rehabilitation professionals who treat neurologic patients with acquired foot deformities. Future studies should model the causes of EVFD, including the TA–EDL imbalance, based on gait analysis data performed with sEMG of the limb muscles. More sophisticated models could also be used to evaluate the effect of specific muscle activation patterns and muscle rheological alterations on lower limb kinematics.

Supplementary Materials: The following supporting information can be downloaded at: <https://www.mdpi.com/article/10.3390/app13137984/s1>, Data S1: Data and computation; Table S1: Mechanical parameters of the foot ligaments adopted in the model.

Author Contributions: Conceptualization, D.M. and C.A.F.; methodology and software, C.A.F. and C.B.; writing—original draft preparation, C.A.F., D.M. and A.M.; writing—review and editing, C.A.F., A.M., D.M. and C.B.; visualization, C.A.F.; supervision, D.M. All authors have read and agreed to the published version of the manuscript.

Funding: This research received no external funding.

Institutional Review Board Statement: Not applicable.

Informed Consent Statement: Not applicable.

Data Availability Statement: Not applicable.

Conflicts of Interest: The authors declare no conflict of interest.

References

1. Inzitari, D.; Carlucci, G. Italian Stroke Guidelines (SPREAD): Evidence and clinical practice. *Neurol. Sci.* **2006**, *27*, s225–s227. [[CrossRef](#)] [[PubMed](#)]
2. Lim, K.B.; Kim, J.-A. Activity of Daily Living and Motor Evoked Potentials in the Subacute Stroke Patients. *Ann. Rehabil. Med.* **2013**, *37*, 82–87. [[CrossRef](#)] [[PubMed](#)]
3. Moura Rde, C.; Fukujima, M.M.; Aguiar, A.S.; Fontes, S.V.; Dauar, R.F.; Prado, G.F. Predictive factors for spasticity among ischemic stroke patients. *Arq. Neuropsiquiatr.* **2009**, *67*, 1029–1036. [[CrossRef](#)] [[PubMed](#)]
4. Lundström, E.; Smits, A.; Terént, A.; Borg, J. Time-course and determinants of spasticity during the first six months following first-ever stroke. *J. Rehabil. Med.* **2010**, *42*, 296–301. [[CrossRef](#)] [[PubMed](#)]
5. Urban, P.P.; Wolf, T.; Uebele, M.; Marx, J.J.; Vogt, T.; Stoeter, P.; Bauermann, T.; Weibrich, C.; Vucurevic, G.D.; Schneider, A.; et al. Occurrence and Clinical Predictors of Spasticity after Ischemic Stroke. *Stroke* **2010**, *41*, 2016–2020. [[CrossRef](#)]
6. Wissel, J.; Schelosky, L.D.; Scott, J.; Christe, W.; Faiss, J.H.; Mueller, J. Early development of spasticity following stroke: A prospective, observational trial. *J. Neurol.* **2010**, *257*, 1067–1072. [[CrossRef](#)]
7. Ryu, J.S.; Lee, J.W.; Lee, S.I.; Chun, M.H. Factors Predictive of Spasticity and Their Effects on Motor Recovery and Functional Outcomes in Stroke Patients. *Top. Stroke Rehabil.* **2010**, *17*, 380–388. [[CrossRef](#)]
8. de Haart, M.; Geurts, A.C.; Huijdekoper, S.C.; Fasotti, L.; van Limbeek, J. Recovery of standing balance in postacute stroke patients: A rehabilitation cohort study. No commercial party having a direct financial interest in the results of the research supporting this article has or will confer a benefit upon the author(s) or upon any organization with which the author(s) is/are associated. *Arch. Phys. Med. Rehabil.* **2004**, *85*, 886–895. [[CrossRef](#)]
9. Keenan, M.A.; Perry, J.; Jordan, C. Factors affecting balance and ambulation following stroke. *Clin. Orthop. Relat. Res.* **1984**, *182*, 165–171. [[CrossRef](#)]
10. Edwards, P.; Hsu, J. SPLATT Combined with Tendo Achilles Lengthening for Spastic Equinovarus in Adults: Results and Predictors of Surgical Outcome. *Foot Ankle* **1993**, *14*, 335–338. [[CrossRef](#)]
11. Lawrence, S.J.; Botte, M.J. Management of the Adult, Spastic, Equinovarus Foot Deformity. *Foot Ankle Int.* **1994**, *15*, 340–346. [[CrossRef](#)] [[PubMed](#)]
12. Hebel, N.; Keenan, M. Neuro-orthopedic management of the dysfunctional extremity in upper motor neuron syndromes. *Eur. J. Phys. Rehabil. Med.* **2004**, *40*, 145.
13. Giannotti, E.; Merlo, A.; Zerbinati, P.; Prati, P.; Masiero, S.; Mazzoli, D. Safety and long-term effects on gait of hemiplegic patients in equinovarus foot deformity surgical correction followed by immediate rehabilitation: A prospective observational study. *Eur. J. Phys. Rehabil. Med.* **2019**, *55*, 169–175. [[CrossRef](#)]
14. Gage, J. Gait analysis. An essential tool in the treatment of cerebral palsy. *Clin. Orthop. Relat. Res.* **1993**, *288*, 126–134. [[CrossRef](#)]
15. Vogt, J.C.; Bach, G.; Cantini, B.; Perrin, S. Split anterior tibial tendon transfer for varus equinus spastic foot deformity: Initial clinical findings correlate with functional results: A series of 132 operated feet. *Foot Ankle Surg.* **2011**, *17*, 178–181. [[CrossRef](#)] [[PubMed](#)]
16. King, B.W.; Ruta, D.J.; Irwin, T.A. Spastic foot and ankle deformities: Evaluation and treatment. *Foot Ankle Clin.* **2014**, *19*, 97–111. [[CrossRef](#)]
17. Freire, B.; Abou, L.; Dias, C.P. Equinovarus foot in stroke survivors with spasticity: A narrative review of muscle–tendon morphology and force production adaptation. *Int. J. Ther. Rehabil.* **2020**, *27*, 1–8. [[CrossRef](#)]
18. Kamath, A.F.; Pandya, N.K.; Namdari, S.; Hosalkar, H.S.; Keenan, M.A. Surgical Technique for the Correction of Adult Spastic Equinovarus Foot. *Tech. Foot Ankle Surg.* **2009**, *8*, 160–167. Available online: https://journals.lww.com/techfootankle/Fulltext/2009/12000/Surgical_Technique_for_the_Correction_of_Adult.3.aspx (accessed on 1 February 2023). [[CrossRef](#)]
19. Limpaphayom, N.; Chantarongsuk, B.; Osateerakun, P.; Prasongchin, P. The split anterior tibialis tendon transfer procedure for spastic equinovarus foot in children with cerebral palsy: Results and factors associated with a failed outcome. *Int. Orthop.* **2015**, *39*, 1593–1598. [[CrossRef](#)]
20. Keenan, M.A. The Management of Spastic Equinovarus Deformity Following Stroke and Head Injury. *Foot Ankle Clin.* **2011**, *16*, 499–514. [[CrossRef](#)]

21. Perry, J. The Use of Gait Analysis for Surgical Recommendations in Traumatic Brain Injury. *J. Head Trauma Rehabil.* **1999**, *14*, 116–135. Available online: https://journals.lww.com/headtraumarehab/Fulltext/1999/04000/The_Use_of_Gait_Analysis_for_Surgical.3.aspx (accessed on 1 February 2023). [CrossRef]
22. Waters, R.L.; Perry, J.; Garland, D. Surgical correction of gait abnormalities following stroke. *Clin. Orthop. Relat. Res.* **1978**, *131*, 54–63. [CrossRef]
23. Duchenne, G.B. *Physiology of Motion*; J.B. Lippincott Company: Philadelphia, PA, USA, 1949.
24. Reynard, F.; Dériaz, O.; Bergeau, J. Foot varus in stroke patients: Muscular activity of extensor digitorum longus during the swing phase of gait. *Foot* **2009**, *19*, 69–74. [CrossRef] [PubMed]
25. Deltombe, T.; Wautier, D.; Cloedt, P.; Fostier, M.; Gustin, T. Assessment and treatment of spastic equinovarus foot after stroke: Guidance from the Mont-Godinne interdisciplinary group. *J. Rehabil. Med.* **2017**, *49*, 461–468. [CrossRef]
26. Campanini, I.; Cosma, M.; Manca, M.; Merlo, A. Added Value of Dynamic EMG in the Assessment of the Equinus and the Equinovarus Foot Deviation in Stroke Patients and Barriers Limiting Its Usage. *Front. Neurol.* **2020**, *11*, 583399. [CrossRef]
27. Hosalkar, H.; Goebel, J.; Reddy, S.; Pandya, N.K.; Keenan, M.A. Fixation Techniques for Split Anterior Tibialis Transfer in Spastic Equinovarus Feet. *Clin. Orthop. Relat. Res.* **2008**, *466*, 2500–2506. [CrossRef]
28. Frigo, C.A. Special Issue: Musculoskeletal Models in a Clinical Perspective. *Appl. Sci.* **2021**, *11*, 6250. [CrossRef]
29. Killen, B.A.; Falisse, A.; De Groote, F.; Jonkers, I. In Silico-Enhanced Treatment and Rehabilitation Planning for Patients with Musculoskeletal Disorders: Can Musculoskeletal Modelling and Dynamic Simulations Really Impact Current Clinical Practice? *Appl. Sci.* **2020**, *10*, 7255. [CrossRef]
30. Fregly, B.J. A Conceptual Blueprint for Making Neuromusculoskeletal Models Clinically Useful. *Appl. Sci.* **2021**, *11*, 2037. [CrossRef]
31. Frigo, C.A.; Donno, L. The Effects of External Loads and Muscle Forces on the Knee Joint Ligaments during Walking: A Musculoskeletal Model Study. *Appl. Sci.* **2021**, *11*, 2356. [CrossRef]
32. Tzanetis, P.; Marra, M.A.; Fluit, R.; Koopman, B.; Verdonschot, N. Biomechanical Consequences of Tibial Insert Thickness after Total Knee Arthroplasty: A Musculoskeletal Simulation Study. *Appl. Sci.* **2021**, *11*, 2423. [CrossRef]
33. Valente, G.; Taddei, F.; Leardini, A.; Benedetti, M.G. Effects of Hip Abductor Strengthening on Musculoskeletal Loading in Hip Dysplasia Patients after Total Hip Replacement. *Appl. Sci.* **2021**, *11*, 2123. [CrossRef]
34. Zographos, S.; Chaminade, B.; Hobatho, M.C.; Utheza, G. Experimental study of the subtalar joint axis: Preliminary investigation. *Surg. Radiol. Anat.* **2001**, *22*, 271–276. [CrossRef]
35. Riener, R.; Edrich, T. Identification of passive elastic joint moments in the lower extremities. *J. Biomech.* **1999**, *32*, 539–544. [CrossRef]
36. Trompetto, C.; Currà, A.; Puce, L.; Mori, L.; Serrati, C.; Fattapposta, F.; Abbruzzese, G.; Marinelli, L. Spastic dystonia in stroke subjects: Prevalence and features of the neglected phenomenon of the upper motor neuron syndrome. *Clin. Neurophysiol.* **2019**, *130*, 521–527. [CrossRef] [PubMed]
37. Gracies, J. Pathophysiology of spastic paresis. I: Paresis and soft tissue changes. *Muscle Nerve Off. J. Am. Assoc. Electrodiagn. Med.* **2005**, *31*, 535–551. [CrossRef]
38. Gracies, J. Pathophysiology of spastic paresis. II: Emergence of muscle overactivity. *Muscle Nerve Off. J. Am. Assoc. Electrodiagn. Med.* **2005**, *31*, 552–571. [CrossRef]
39. Mazzoli, D.; Giannotti, E.; Rambelli, C.; Zerbinati, P.; Galletti, M.; Mascioli, F.; Prati, P.; Merlo, A. Long-term effects on body functions, activity and participation of hemiplegic patients in equino varus foot deformity surgical correction followed by immediate rehabilitation. A prospective observational study. *Top. Stroke Rehabil.* **2019**, *26*, 518–522. [CrossRef]
40. Perry, J.; Burnfield, J.M. *Gait Analysis: Normal and Pathological Function*, 2nd ed.; Slack: Thorofare, NJ, USA, 2010.
41. Damiano, D.L.; Prosser, L.A.; Curatalo, L.A.; Alter, K.E. Muscle Plasticity and Ankle Control after Repetitive Use of a Functional Electrical Stimulation Device for Foot Drop in Cerebral Palsy. *Neurorehabil. Neural Repair* **2012**, *27*, 200–207. [CrossRef]
42. Weber, D.J.; Stein, R.B.; Chan, K.M.; Loeb, G.E.; Richmond, F.J.; Rolf, R.; James, K.; Chong, S.L.; Thompson, A.K.; Misiaszek, J. Functional electrical stimulation using microstimulators to correct foot drop: A case study. *Can. J. Physiol. Pharmacol.* **2004**, *82*, 784–792. [CrossRef]
43. Giannotti, E.; Merlo, A.; Zerbinati, P.; Longhi, M.; Prati, P.; Masiero, S.; Mazzoli, D. Early rehabilitation treatment combined with equinovarus foot deformity surgical correction in stroke patients: Safety and changes in gait parameters. *Eur. J. Phys. Rehabil. Med.* **2015**, *52*, 296–303. [PubMed]
44. Kendall, F.P.; McCreary, E.K. *Muscles, Testing and Function*; Williams & Wilkins: Philadelphia, PA, USA, 1983.
45. Kapandji, I.A. *The Physiology of the Joints*; Churchill Livingstone: London, UK, 1987; Volume 2-Lower limb.
46. Bavikatte, G.; Subramanian, G.; Ashford, S.; Allison, R.; Hicklin, D. Early identification, intervention and management of post-stroke spasticity: Expert consensus recommendations. *J. Cent. Nerv. Syst. Dis.* **2021**, *13*, 11795735211036576. [CrossRef] [PubMed]
47. Miller, S.C.; Korff, T.; Waugh, C.; Fath, F.; Blazevich, A.J. Tibialis Anterior Moment Arm: Effects of Measurement Errors and Assumptions. *Med. Sci. Sports Exerc.* **2015**, *47*, 428–439. [CrossRef] [PubMed]
48. Maganaris, C.N. Force-length characteristics of in vivo human skeletal muscle. *Acta Physiol. Scand.* **2001**, *172*, 279–285. [CrossRef] [PubMed]

49. Lenhardt, S.A.; McIntosh, K.C.; Gabriel, D.A. The surface EMG-force relationship during isometric dorsiflexion in males and females. *Electromyogr. Clin. Neurophysiol.* **2009**, *49*, 227.
50. Friederich, J.A.; Brand, R.A. Muscle fiber architecture in the human lower limb. *J. Biomech.* **1990**, *23*, 91–95. [[CrossRef](#)]
51. Campanini, I.; Bò, M.C.; Salsi, F.; Bassi, M.C.; Damiano, B.; Scaltriti, S.; Lusuardi, M.; Merlo, A. Physical therapy interventions for the correction of equinus foot deformity in post-stroke patients with triceps spasticity: A scoping review. *Front. Neurol.* **2022**, *13*, 1026850. [[CrossRef](#)] [[PubMed](#)]
52. Blankevoort, L.; Huiskes, R. Ligament-Bone Interaction in a Three-Dimensional Model of the Knee. *J. Biomech. Eng.* **1991**, *113*, 263–26991. [[CrossRef](#)]
53. Mkandawire, C.; Ledoux, W.; Sangeorzan, B.J.; Ching, R.P. Foot and ankle ligament morphometry. *J. Rehabil. Res. Dev.* **2005**, *42*, 809–820. [[CrossRef](#)]
54. Cheung, J.T.-M.; Zhang, M.; An, K.-N. Effects of plantar fascia stiffness on the biomechanical responses of the ankle-foot complex. *Clin. Biomech.* **2004**, *19*, 839–846. [[CrossRef](#)]
55. Siegler, S.; Block, J.; Schneck, C.D. The Mechanical Characteristics of the Collateral Ligaments of the Human Ankle Joint. *Foot Ankle* **1988**, *8*, 234–242. [[CrossRef](#)] [[PubMed](#)]
56. Gefen, A. The *in Vivo* Elastic Properties of the Plantar Fascia during the Contact Phase of Walking. *Foot Ankle Int.* **2003**, *24*, 238–244. [[CrossRef](#)] [[PubMed](#)]
57. Martelli, S.; Valente, G.; Viceconti, M.; Taddei, F. Sensitivity of a subject-specific musculoskeletal model to the uncertainties on the joint axes location. *Comput. Methods Biomech. Biomed. Eng.* **2014**, *18*, 1555–1563. [[CrossRef](#)] [[PubMed](#)]

Disclaimer/Publisher’s Note: The statements, opinions and data contained in all publications are solely those of the individual author(s) and contributor(s) and not of MDPI and/or the editor(s). MDPI and/or the editor(s) disclaim responsibility for any injury to people or property resulting from any ideas, methods, instructions or products referred to in the content.